European Journal of Radiology 195 (2026) 112643

Contents lists available at ScienceDirect

European Journal of Radiology

journal homepage: www.elsevier.com/locate/ejrad

Development and characterization of new contrast agents for Photon-Counting CT

Mika Donabauer [a,b], Stefan Sawall [c], Isabelle Ayx [d], Carmen Wängler [b,e,*], Stefan O. Schoenberg [b,d], Björn Wängler [a,b,f,*]

[a] Molecular Imaging and Radiochemistry, Clinic of Radiology and Nuclear Medicine, Medical Faculty Mannheim, Heidelberg University, Mannheim, Germany
[b] Research Campus M2OLIE, Medical Faculty Mannheim, Heidelberg University, Mannheim, Germany
[c] Division of X–Ray Imaging and CT, German Cancer Research Center (DKFZ), Heidelberg, Germany
[d] Clinic of Radiology and Nuclear Medicine, University Medical Center Mannheim, Heidelberg University, Mannheim, Germany
[e] Biomedical Chemistry, Clinic of Radiology and Nuclear Medicine, Medical Faculty Mannheim, Heidelberg University, Mannheim, Germany
[f] Mannheim Institute for Intelligent Systems in Medicine (MIISM), Medical Faculty Mannheim, Heidelberg University, Mannheim Germany

ARTICLE INFO

Keywords:
Photon-Counting CT (PCCT)
Contrast Agents
Phantom
Imaging
X-ray attenuation

ABSTRACT

Purpose: The development of novel contrast agents is a critical step in unleashing the full potential of Photon-Counting Computed Tomography (PCCT), as clinically approved iodine contrast agents do not exhibit optimal spectral properties to harness the full potential of photon-counting detectors. Moreover, material decomposition requires the application of different contrast agents with differing X-ray attenuation characteristics at different photon energies. However, the development of contrast agents being suitable for this purpose is in its infancy, limiting the imaging options of PCCT. In this study, we investigated which of the elements lanthanum, gadolinium, ytterbium, lead, bismuth and gold are suitable for use as the basis of contrast agents in PCCT as these should exhibit highly interesting X-ray attenuation characteristics at different tube voltages for this application.
Methods: New contrast agents based on the aforementioned elements were synthesized and characterized in terms of stability. Further, these substances were characterized by phantom studies on the first FDA-approved clinical PCCT Naeotom Alpha scanner with regard to contrast generation at different tube voltages of 70, 90, 120, and 140 kV in comparison to the approved iodine-based contrast agent Gastrolux to determine their general potential for PCCT imaging.
Results: We found that at lower tube voltages of 70 kV, iodine (48.1 ± 0.8 HU/(mg/mL)) and gadolinium (43.5 ± 1.0 HU/(mg/mL)) demonstrated the highest attenuation rates, whereas lanthanum, gold, ytterbium, and lead showed lower X-ray attenuation efficiency under these conditions (35.7 ± 0.7, 28.1 ± 0.6, 25.8 ± 0.2, and 25.3 ± 0.1 HU/(mg/mL), respectively). At a higher tube voltage of 120 kV, the situation changed, showing the highest attenuation rates for gadolinium, ytterbium, and iodine (33.4 ± 0.4, 28.1 ± 0.1, and 24.6 ± 0.3 HU/(mg/mL), respectively), followed by gold, bismuth, lanthanum, and lead (23.5 ± 0.3, 21.7 ± 0.2, 19.7 ± 0.3, and 18.1 ± 0.1 HU/(mg/mL), respectively).
Conclusions: Although all elements investigated showed a general suitability for implementation in contrast-enhanced CT imaging, iodine, gadolinium and ytterbium demonstrated the highest potential in this regard. However, also gold and bismuth could in general be suitable for material decomposition studies in combination with the aforementioned elements in cases necessitating a strongly varying contrasting behavior at chosen tube voltages.

1. Introduction

The visualization and characterization of benign and malignant structures using computed tomography (CT) is an integral part of clinical routine and thus, CT is one of the most important non-invasive imaging modalities available today [1–4]. The number of CT scans

* Corresponding authors at: Medical Faculty Mannheim, Clinic of Radiology and Nuclear Medicine, Biomedical Chemistry, Theodor-Kutzer-Ufer 1–3, 68167 Mannheim, Germany.
E-mail addresses: Carmen.Waengler@uni-heidelberg.de (C. Wängler), Bjoern.Waengler@medma.uni-heidelberg.de (B. Wängler).

https://doi.org/10.1016/j.ejrad.2025.112643
Received 2 September 2025; Received in revised form 24 November 2025; Accepted 31 December 2025
Available online 31 December 2025

performed each year is approximately 300 million with an annual growth rate of 4 % [1]. A disadvantage of the current CT imaging technology, however, is the detection of the X-rays, which is conventionally performed using energy-integrating detectors (EIDs). Signals in EIDs are however dominated by high energy X-ray photons resulting in a loss of contrast [5–7]. Novel Photon-Counting Computed Tomography (PCCT) uses Photon-Counting Detectors (PCDs) that replace the classic scintillators with semiconductors, allowing for the actual counting of single photons and a quantification of their energy [8,9]. In addition, PCCT provides a higher spatial resolution due to smaller PCD units compared to EIDs [10,11]. Furthermore, photons are usually sorted in energy bins, facilitating dual- and multi-energy acquisitions with a single detector. By this, PCCT in principle enables several different contrast agents to be used simultaneously and to be differentiated by so-called material decomposition. This enables different structures or contrast agents to be distinguished and characterized at the same time, e.g. exogenous contrast agents from soft tissue and calcium-containing structures, thus enabling a new class of functional imaging [12–15]. One potential clinical application for the combinatorial use of two contrast agents is e.g. in cardiac imaging where iodine-based agents could be used during coronary CT angiography for the visualization of the coronary arteries whereas a heavy element-based counterpart could be applied for texture analysis of the left ventricular myocardium within one scan, resulting in a considerable dose reduction and higher time efficiency. This methodology could also be implemented in the characterization of tumor diseases. As well, the simultaneous depiction of arterial and venous systems is a potential application field for this approach [16].

Despite the high clinical potential of this methodology, it is currently not fully applicable as it requires the use of multiple contrast agents being based on different elements, exhibiting different k-edges and thus X-ray attenuation characteristics at different photon energies [16,17]. The conventional iodine- and barium-based contrast agents exhibit a limited suitability for this purpose as they do not optimally attenuate the X-rays of the clinical imaging systems in all energy ranges due to their k-edges of 33.2 keV and 37.4 keV, respectively, lying at one end of the applied photon spectrum. Thus, it would be advantageous to involve heavier elements for photon attenuation which exhibit k-edges and thus optimal X-ray attenuation characteristics at higher energies of around 40–100 keV to cover the whole clinically applied photon energy spectrum (Fig. 1A).

Thus, new contrast agents have to be developed which meet several key criteria to unleash the full potential of PCCT enabling material decomposition and k-edge imaging. These criteria include cost efficiency, sufficient annual production of the educts and, most importantly, k-edges of the used elements that lie within the clinically applied X-ray spectrum (Fig. 1). In this regard, the elements lanthanum, gadolinium, ytterbium, lead, gold, and bismuth are of high interest for the development of new contrast agents as they exhibit k-edges ranging from 38.9 keV for lanthanum to 90.5 keV for lead, covering the full range of the clinically relevant energy spectrum [19,20].

Although there are studies describing the use of other elements than iodine and barium such as tungsten, tantalum or bismuth for PCCT imaging, demonstrating in some cases principal suitability for PCCT and material decomposition, these have been used in pure form which would result in a high toxicity when applied to humans or use heavy elements-based contrast agents in the form of nanoparticles [11,16,19,21–24]. Human application of such nanoparticle systems is however often controversially discussed with regard to their long-time fate and associated toxicity after application, making small molecule-based imaging agents preferable as their biodistribution profile and clearance from the human body are well known.

Although lanthanum, gadolinium, ytterbium, lead, and bismuth should have a high potential for application in PCCT, their use in CT or PCCT imaging is limited as these elements also exhibit an intrinsic high toxicity which prevents their use in free form [25,26]. This limitation can however in principle be efficiently overcome by chelation analogously to gadolinium being used in magnetic resonance imaging (MRI) [27]. Among the above-mentioned highly promising elements for PCCT, gold is the only exception as this highly inert metal does not exhibit a relevant toxicity, cannot be complexed but can be applied in form of nanoparticles with fast clearing properties [28,29].

In order to solve the above-mentioned limitations caused by the lack of appropriate contrast agents and thus enable the full potential of PCCT to be exploited, we developed and characterized in this study different new agents based on the most promising elements gadolinium, ytterbium, gold, lead and bismuth and investigated their stability and thus general suitability for in vivo application. The most stable agents were in the following studied with regard to contrast generation and thus their potential for use in PCCT on the first and currently only FDA-approved whole-body Naeotom Alpha PCCT system using the iodine-based agent Gastrolux as the reference.

A

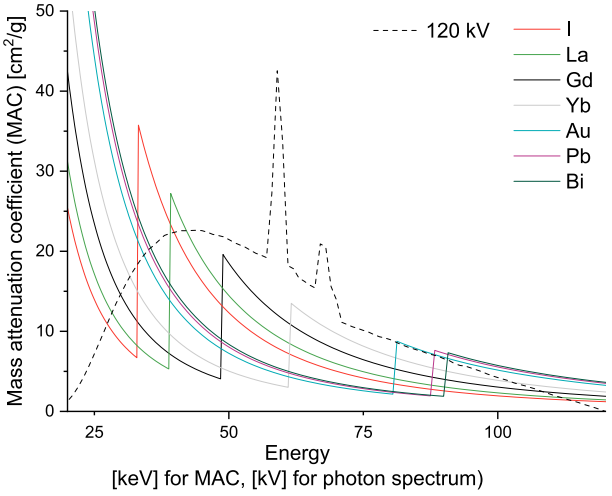

B

Material	Symbol	Atomic number	k-edge (theory, [keV])	Raw cost per 30 g [USD])	Annual production [tons]
Iodine	I	53	33.17	<1	>30,000
Lanthanum	La	57	38.92	<1	12,000
Gadolinium	Gd	64	50.24	<1	400
Ytterbium	Yb	70	61.33	<1	50
Gold	Au	79	80.72	>1000	2800
Lead	Pb	82	88.00	<1	4,500,000
Bismuth	Bi	83	90.53	<1	8500

Fig. 1. (A) Mass attenuation coefficient curves of the elements iodine (I), lanthanum (La), gadolinium (Gd), ytterbium (Yb), gold (Au), lead (Pb) and bismuth (Bi) and CT X-ray spectrum at a tube voltage of 120 kV. The X-ray photon spectrum (dotted line) was generated with the Matlab toolkit "Spektr". The mass attenuation coefficient data for the different elements were taken from the database nist.gov (solid lines).[18] (B) Comparison of the most important characteristics of iodine and the heavy elements lanthanum, gadolinium, ytterbium, gold, lead and bismuth being of particular interest as basis for CT contrast agent development.

Such studies on stable low molecular weight contrast agents based on the mentioned elements have not been reported so far but are the mandatory prerequisite for the clinical translation of material decomposition PCCT imaging in patients using heavy elements.

2. Methods

2.1. Contrast agents

General information about chemicals and instrumentation used for syntheses and analyses, purification and characterization of LaDOTA, GdDOTA, YbDOTA, PbDOTAM, BiDOTAM and coated gold nanoparticles as well as a detailed description of the preparation and the analysis of the agents can be found in the supplemental information (DOTA: (2,2′,2″,2‴-(1,4,7,10-tetraazacyclododecane-1,4,7,10-tetrayl) tetraacetic acid); DOTAM: (2-[4,7,10-tris(2-amino-2-oxoethyl)-1,4,7,10-tetrazacyclododec-1-yl]acetamide)).

Briefly, the preparation of the DOTA complexes (Fig. 2A) was accomplished using an optimized protocol: DOTA and the respective metal ion salt (1.1 eq.) were dissolved in H_2O, the pH was adjusted to 5.5 and the resulting mixture heated to 70 °C for 24 h. The metal excess was removed by chelation and the respective products obtained in high yields of 96–98 %. In contrast, the DOTAM complexes (Fig. 2A) were obtained by using 1 eq. of the respective metal salt in methanol:H_2O (8:2, *v/v*) as the solvent within 2 h of refluxing, precipitation and recrystallization in yields of 77–89 %. All small molecule-based contrast agents were obtained in purities of ≥ 95 % and their chemical identity was confirmed by high-resolution mass spectrometry (Fig. S1 – S5) and nuclear magnetic resonance (NMR) spectroscopy (Fig. S6 and S7). For the synthesis of the gold nanoparticles (Fig. 2B), a published procedure was adapted, giving silica-coated, small nanoparticles of 3.5 ± 1.5 nm size in high reproducibility, being characterized by NMR (Fig. S8), X-ray

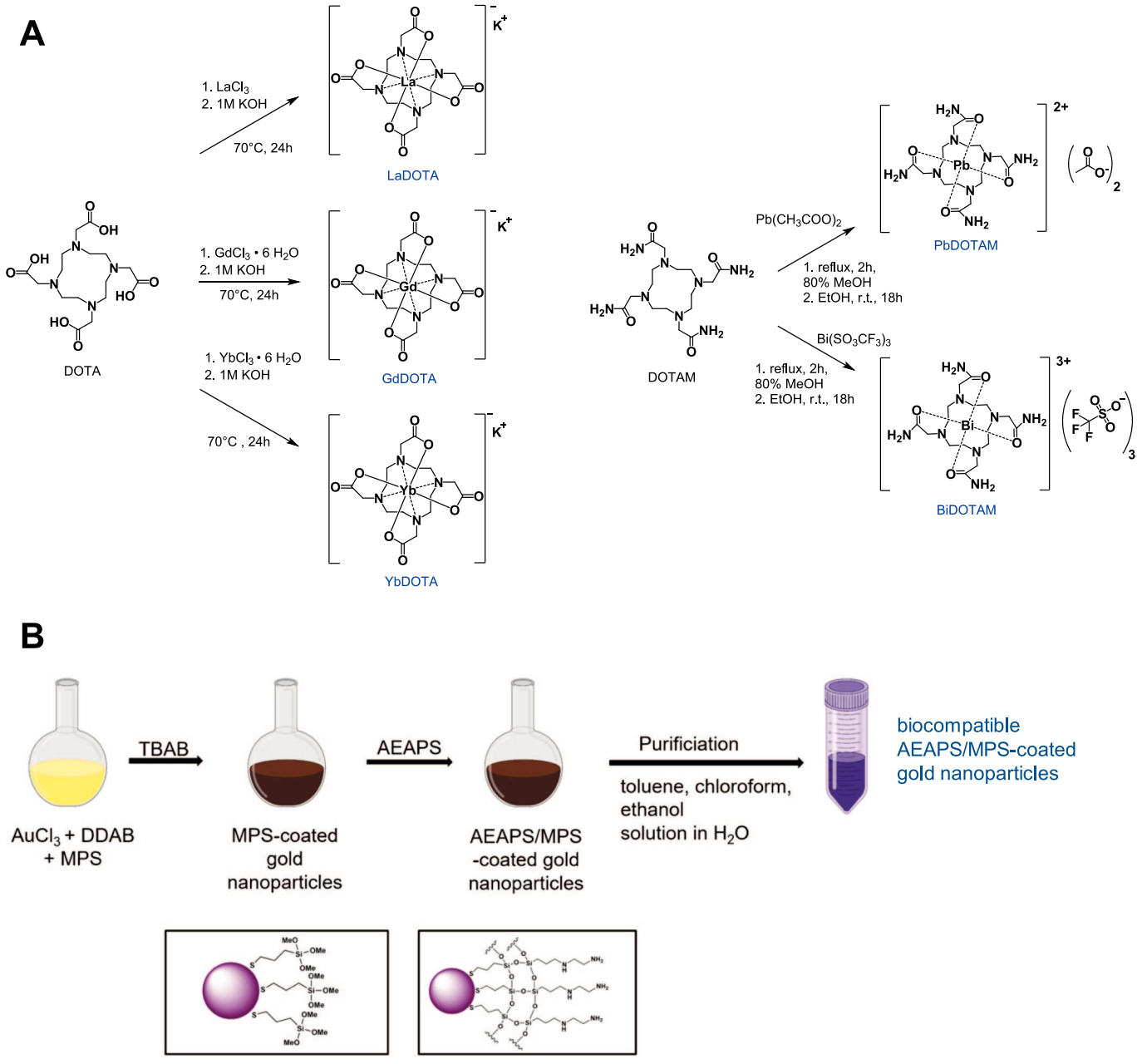

Fig. 2. Schematic depiction of the synthesis pathways giving the contrast agents LaDOTA, GdDOTA, YbDOTA, PbDOTAM, BiDOTAM (**A**), and the silica-coated gold nanoparticles (**B**). Details of the synthetic procedures as well as results of chemical characterization analyses can be found in the supplementary material.

diffraction (XRD) (Fig. S9), UV/Vis absorption (Fig. S10), and infrared (IR) spectroscopy (Fig. S11) [30].

2.2. Phantom setup and concentration series of the contrast agents

A cylindrical poly(methyl methacrylate) (PMMA) phantom with a diameter of 10 cm and eight cylindrical compartments was used to evaluate the CT contrast properties of all agents. Contrast agent solutions were prepared in 5 mL vials by dissolving LaDOTA, GdDOTA, YbDOTA, PbDOTAM, BiDOTAM and coated gold nanoparticles in contrasting element concentrations of 0, 5, 10, 15, 20, 25, 30, and 35 mg/mL in water and afterwards transferred to the compartments of the phantom. Pure water was also filled in one compartment for normalization and the compartments were sealed with stoppers. The phantom was placed horizontally on the head piece of the examination bed and measured at ambient temperature using an abdomen protocol with 0.25 s rotation time, 1.2 pitch, and 144 x 0.4 mm collimation. For every applied voltage, the concentration series was measured three times in independent experiments. To determine the CT-value, a circular ROI (region of interest) was drawn in a coronal slice showing each tube. CT-values, in the following referred to as mean attenuation values, were recorded in Hounsfield units (HU). The HU values were read out using the system's internal software and from these, the attenuation rates – describing the attenuation (in HU units) of the contrast agent per mass concentration (in mg/mL) – were obtained, enabling the direct comparison of the achievable contrasts of the respective elements.

2.3. CT images

Phantom images were acquired on a Naeotom Alpha PCCT system (Siemens Healthineers, Forchheim, Germany, Fig. 3) to evaluate the CT-values of all synthesized contrast agents. Acquisitions were performed using all available tube voltages (70 kV, 90 kV, 120 kV, and 140 kV), using the maximum available dose possible at each tube voltage. Tube current modulation was disabled to reduce the number of confounding factors. Image reconstruction was performed using a 512 x 512 voxel matrix with a slice thickness of 3.0 mm as well as increment of 3.0 mm since the vials are invariant in the z-direction using a quantitative Qr44 kernel. As T3D images were generated, all photons were reconstructed together over the corresponding energy range.

2.4. Image analyses

Attenuation rates (AR) were defined as the attenuation divided by the concentration of the corresponding element in mg/mL, given in HU/(mg/mL) ± standard deviation. By plotting the CT-values (y-axis) against the mass concentration (x-axis) followed by linear regression, the attenuation rate can be determined by the slope of the linear fit (OriginPro 2023 (64-bit) 10.0.0.154).

3. Results

3.1. Development, chemical and physical characterization of the new contrast agents

As outlined before, small molecule-based contrast agents of the elements lanthanum, gadolinium, ytterbium, lead, and bismuth together with the chelating agents DOTA and DOTAM as well as coated gold nanoparticles are of special interest for use in PCCT imaging and were thus first synthesized and characterized.

For the preparation of the DOTA and DOTAM complexes of lanthanum, gadolinium, ytterbium, lead and bismuth, an optimized synthesis strategy was employed, giving all small molecule-based contrast agents in high purities after purification. The identity of the contrast agents was confirmed by high-resolution mass spectrometry and NMR spectroscopy. The gold nanoparticles were obtained in high reproducibility in silica-coated form within the target size range of 3.5 ± 1.5 nm size and characterized by NMR, XRD, UV/Vis absorption, and IR spectroscopy. The small size of the particles enables an efficient excretion by the renal pathway which is favorable with regard to a rapid and complete clearance from the organism [31]. The silica coating is essential on the one hand for biocompatibility but also for the high

Parameter	Specification
Platform	Naeotom Alpha
X-ray tubes	2 Vectron® X-ray tubes
Detector	2 QuantaMax CT detectors with quantum counting
Max. number of acquired slices	2 x 144 slices
Max. number of reconstructed slices	2 x 288 slices
mA	Up to 1,300 mA
Temporal resolution	Up to 66 ms
kV	70, 90, 100, 120, 140 kV Sn100, Sn140 kV
Coverage in z-direction	144 x 0.4 mm 120 x 0.2 mm (Quantum HD)
Spatial resolution	0.11 mm (in the plane) in UHR mode
Power	2 x 120 kW
Load capacity of the table	Up to 307 kg
Table speed	Up to 737 mm/s (with Turbo Flash)

Fig. 3. Specifications of the clinical PCCT Naeotom Alpha system used for the PCCT measurements in this study.

stability of the systems, as non-coated nanoparticles were observed to aggregate within weeks. In contrast, the silica-coated nanoparticles were continuously monitored over the period of one year regarding stability and aggregation, with no adverse observations made.

The chelators DOTA and DOTAM were chosen due to the superior stability of their complexes compared to acyclic agents [32,33] and the corresponding complexes of each element were in the following studied in direct comparison with regard to stability. These studies demonstrated that for lanthanum, gadolinium and ytterbium, the complexes with DOTA were of comparably high stability and considerably more stable than those with the ligand DOTAM. In contrast, DOTAM was found to produce complexes of higher stability with the elements lead and bismuth compared to DOTA, also resulting in stabilities comparable to approved agents (details on relative kinetic inertness and crystal structures of the complexes will be published elsewhere). This indicates the biocompatibility of the complexes developed here since they show a comparably high stability as clinically applied agent Dotarem and similar approved MRI contrast agents. Thus, there are no fundamental concerns about their use in humans, even though the biocompatibility and toxicity of the agents would have to be thoroughly investigated prior to a clinical application.

Thus, LaDOTA, GdDOTA, YbDOTA, PbDOTAM, and BiDOTAM (Fig. 4A) demonstrated the highest potential for future in vivo use and were in the following – besides the silica-coated gold nanoparticles developed (Fig. 4B) – characterized regarding their X-ray attenuation characteristics by PCCT imaging.

3.2. Characterization of the newly developed contrast agents by PCCT phantom imaging

To determine those of the newly developed agents having the highest potential for use in PCCT imaging in terms of achievable contrasts at different energies, phantom images were acquired on a clinical Naeotom Alpha PCCT system.

For this purpose, the eight chambers of the phantom (Fig. 5A) were filled with a concentration series of the respective contrast agents in water ranging from 0 mg/mL (pure water for normalization purposes) to 35 mg/mL related to the contrasting element. In order to cover the clinical X-ray spectrum, measurements were taken at all available X-ray tube voltages of 70, 90, 120, and 140 kV. The approved iodine-based contrast agent Gastrolux was studied under the same conditions as reference. Exemplary PCCT images of the measurements of the contrast agent concentration series of Gastrolux, LaDOTA, GdDOTA, YbDOTA, gold nanoparticles, PbDOTAM and BiDOTAM at a tube voltage of 120 kV are depicted in Fig. 5B.

The attenuations measured for the different contrast agents increased with increasing concentrations of the respective agent and the element-specific attenuation also changed depending on the tube voltage (Fig. 6B).

For all agents, the linear correlations between measured attenuations and element concentrations were plotted, giving the attenuation rates for the concentrations of the different elements at the differing tube voltages (Fig. 7). The results obtained from linear regression are in good agreement with other studies [19,21] with R^2 values being close to unity (see Table S1 for details). Further, the differences in attenuation rates at different tube voltages were statistically analyzed by ANOVA and Post-hoc tests, showing highly significant differences between slopes ($p < 0.001$) and thus materials. The only exemptions were between gold nanoparticles (Au-NP) – BiDOTAM at 90 kV ($p \approx 0.4237$) and LaDOTA – PbDOTAM at 140 kV ($p \approx 0.1456$). Details of these analyses can be found in the supplementary information (see Table S2).

At a tube voltage of 70 kV, iodine showed the highest attenuation rate of 48.1 ± 0.8 HU/(mg/mL), followed by gadolinium (43.5 ± 1.0 HU/(mg/mL)), lanthanum (35.7 ± 0.7 HU/(mg/mL)) and bismuth (31.2 ± 0.2 HU/(mg/mL)). Although the k-edge of bismuth does not lie within the X-ray photon spectrum at this tube voltage, this element still shows a good attenuation rate (31.2 ± 0.2 HU/(mg/mL)). In contrast, gold and lead attenuated the photons comparably weakly (28.1 ± 0.6 HU/(mg/mL) for Au and 25.3 ± 0.1 HU/(mg/mL) for Pb, respectively). As well, ytterbium, although presenting a k-edge being in principle within the X-ray photon spectrum, also attenuated the radiation relatively weakly (25.8 ± 0.2 HU/(mg/mL). Thus, iodine and gadolinium displayed a 1.39–1.90-fold higher attenuation than the heavy elements Au, Pb and Bi at this tube voltage.

At a tube voltage of 90 kV, the situation changed with gadolinium, demonstrating the highest attenuation with a rate of 41.1 ± 0.6 HU/(mg/mL), followed by iodine (34.5 ± 0.5 HU/(mg/mL)) and ytterbium (28.9 ± 0.3 HU/(mg/mL)). In contrast, iodine and lanthanum (34.5 ± 0.5 HU/(mg/mL) and 26.5 ± 0.4 HU/(mg/mL), respectively) decreased in attenuation efficiency. The heavy elements continued to give the lowest attenuation rates (22.0 ± 0.4 HU/(mg/mL) for gold, 17.9 ± 0.1 HU/(mg/mL) for lead, and 22.4 ± 0.3 HU/(mg/mL) for bismuth). Gadolinium thus demonstrated a 1.83–2.30-fold higher attenuation rate compared to the heavy elements Pb, Au and Bi and a 1.19-fold higher

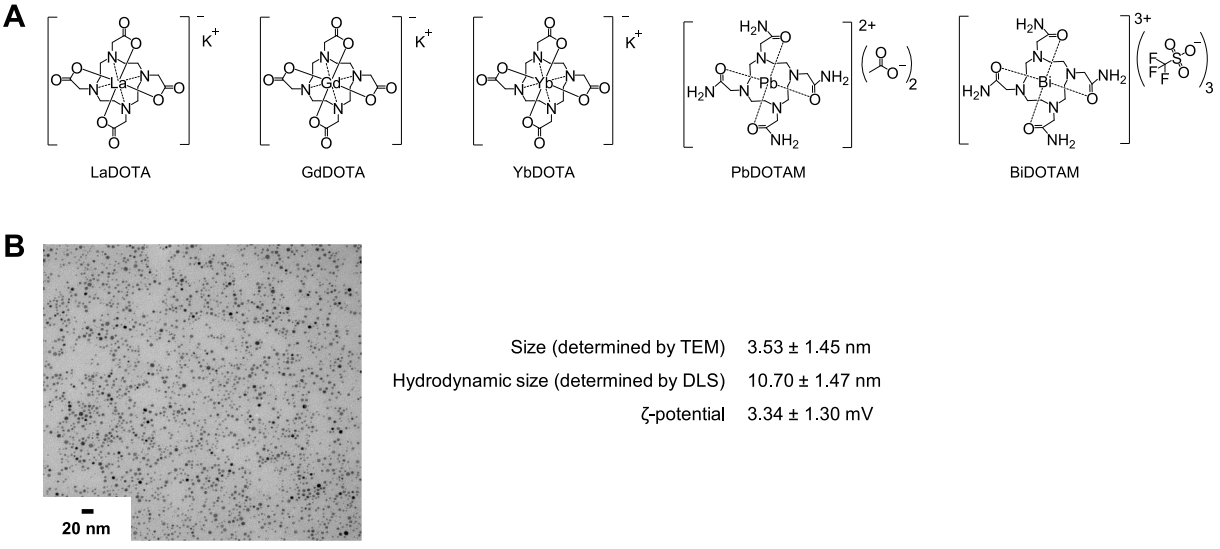

Fig. 4. Structures of the most stable developed contrast agents based on the elements lanthanum, gadolinium, ytterbium, lead, and bismuth (**A**). Transmission electron microscopy (TEM) image and physical parameters of the silica-coated gold nanoparticular contrast agent developed (**B**).

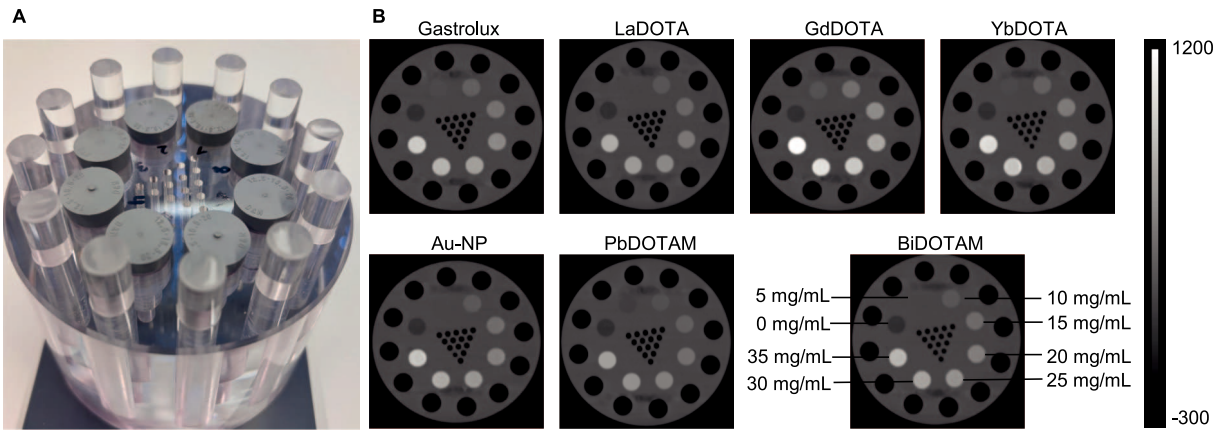

Fig. 5. (**A**) Phantom used in the PCCT measurement series. (**B**) Exemplary depiction of the imaging results of the concentration series of all contrast agents at a tube voltage of 120 kV.

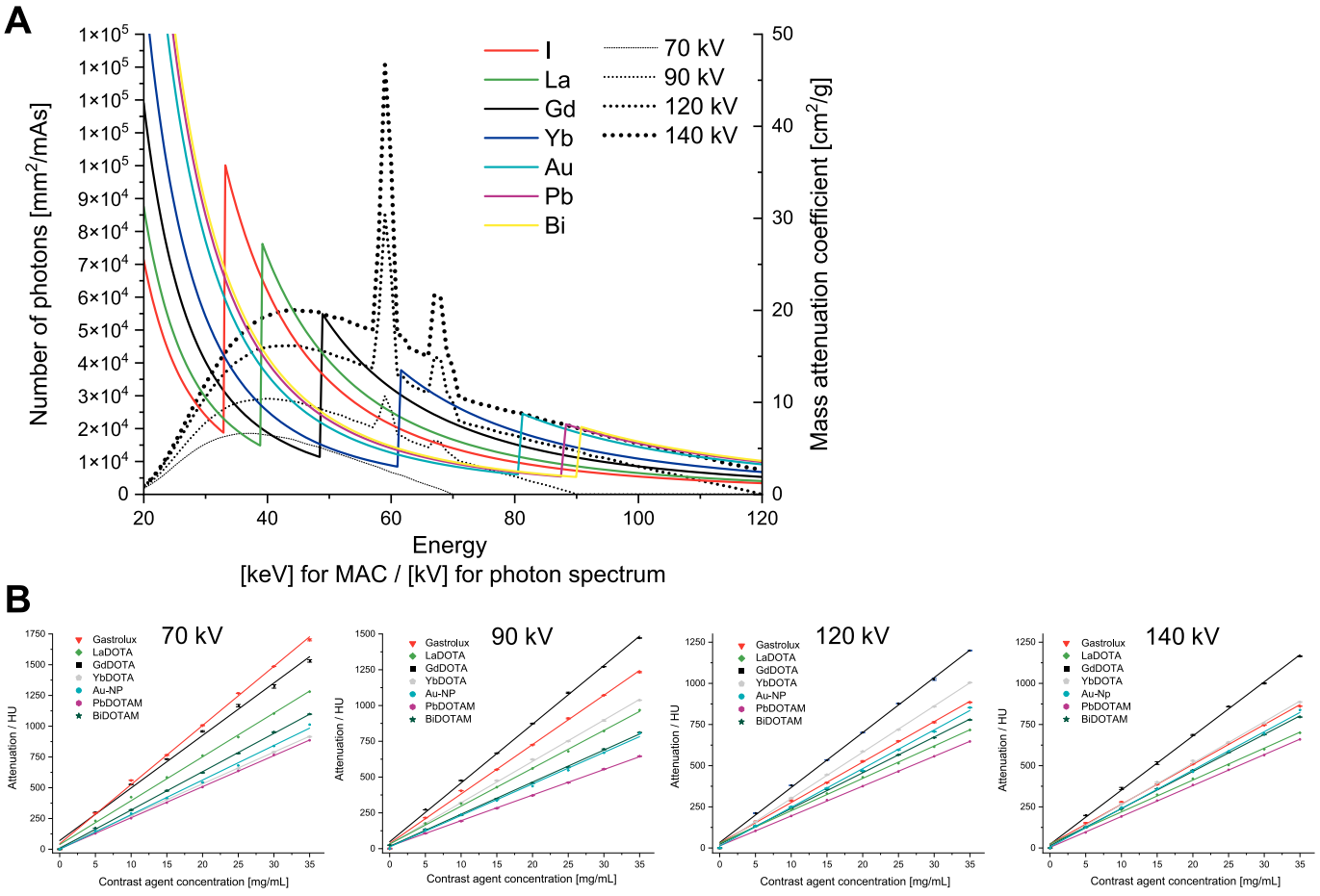

Fig. 6. Mass attenuation coefficients of the elements iodine, lanthanum, gadolinium, ytterbium, gold, lead, and bismuth (solid lines; taken from the nist.gov database [18]) overlaid with the X-ray photon spectra at tube voltages of 70, 90, 120, and 140 kV (dotted lines; generated using the Matlab toolkit "Spektr"; as the exact intrinsic and extrinsic pre-filtering parameters of the used scanner are not known, the simulation of the X-ray photon spectra is not exact and thus should not be interpreted quantitatively but only serves for illustration purposes) (A). Attenuation rates were obtained from the shown plots of measured attenuations against the concentrations of the respective heavy element at tube voltages of 70, 90, 120, and 140 kV and linear regression of the data (B).

attenuation rate compared to iodine at this tube voltage.

At a tube voltage of 120 kV, gadolinium again exhibited the best contrasting properties with an attenuation rate of 33.4 ± 0.4 HU/(mg/mL), being 1.36-fold higher than that of iodine (24.6 ± 0.3 HU/(mg/mL)), followed by ytterbium 28.1 ± 0.1 HU/(mg/mL). In contrast, iodine (24.6 ± 0.3 HU/(mg/mL)), gold (23.5 ± 0.3 HU/(mg/mL)), bismuth (21.7 ± 0.2 HU/(mg/mL)), lanthanum (19.7 ± 0.3 HU/(mg/mL)) and lead (18.1 ± 0.1 HU/(mg/mL)) displayed significantly lower attenuation rates.

At a tube voltage of 140 kV, gadolinium still demonstrated the best contrasting properties with an attenuation rate of 32.9 ± 0.4 HU/(mg/mL), being 1.35-fold higher than that of iodine (24.2 ± 0.3). The second

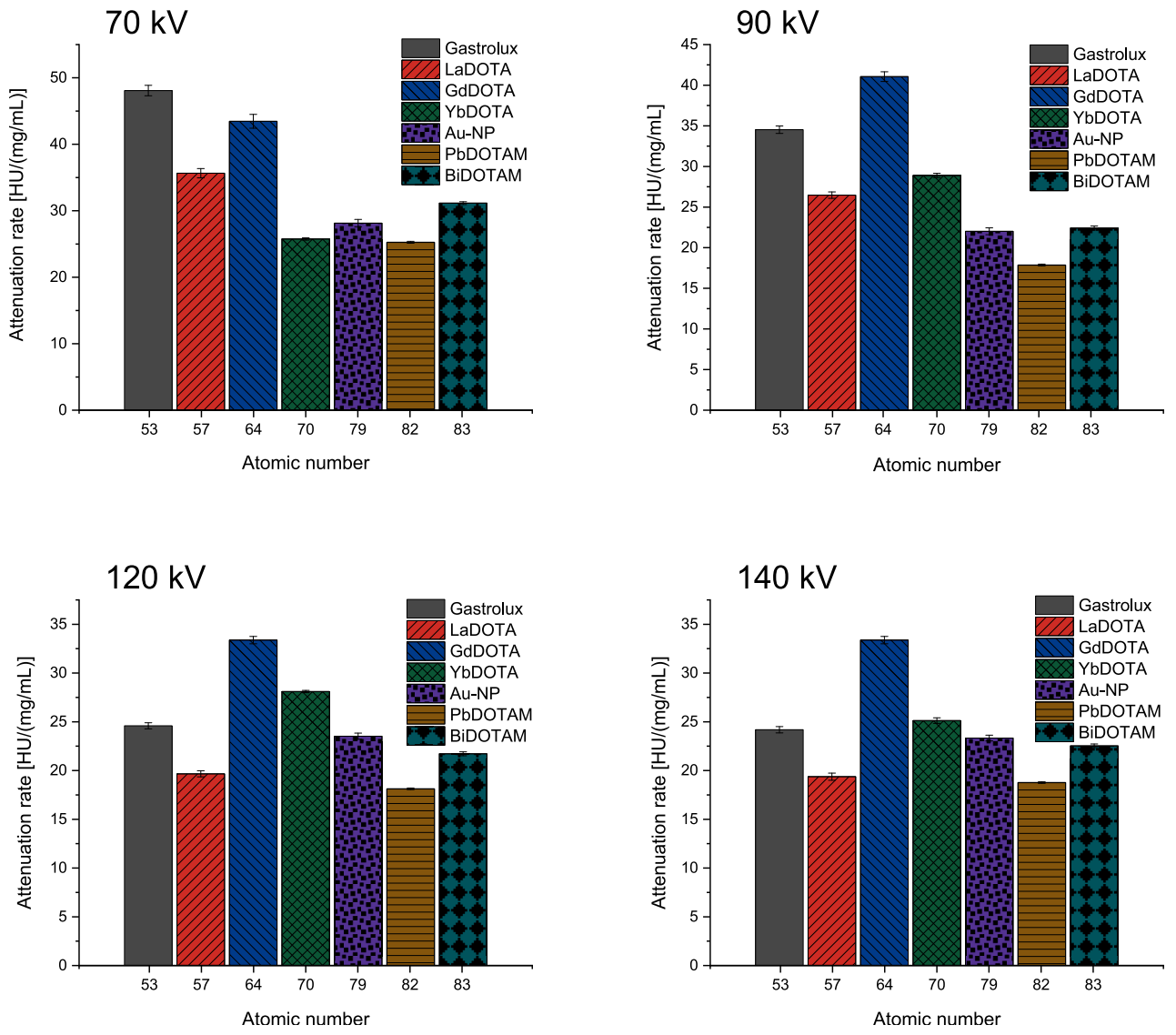

Fig. 7. Attenuation rates of the contrast agents studied here as function of their atomic number (Z) at tube voltages of 70 kV, 90 kV, 120 kV, and 140 kV. All experiments were performed thrice in independent experiments. Error bars depict standard deviations from the mean.

highest attenuation rate was displayed by ytterbium (25.1 ± 0.3 HU/(mg/mL)) with an approximately 1.31-fold lower attenuation rate in comparison to gadolinium. The elements Au, Yb, I and Bi gave similar attenuation rates of 23.3 ± 0.3 HU/(mg/mL), 25.1 ± 0.3 HU/(mg/mL), 24.2 ± 0.3 HU/(mg/mL), and 22.5 ± 0.2 HU/(mg/mL), respectively. Lanthanum (19.4 ± 0.4 HU/(mg/mL)) and lead (18.8 ± 0.1 HU/(mg/mL)) showed the lowest attenuation rates, albeit increasing with higher tube voltages in case of lead.

4. Discussion

Regarding the determination of the attenuation properties of the developed contrast agents at the different tube voltages, the attenuations measured for the different contrast agents increased with increasing concentrations of the respective agent and the element-specific attenuation also changed depending on the tube voltage used (Fig. 6B) due to changed interaction profiles of the elements with X-rays at a certain tube voltage (Fig. 6A).

At 70 kV, iodine demonstrated the highest attenuation rate, followed by gadolinium and lanthanum, being attributable to the fact that these elements exhibit k-edges close to the effective energy of the used spectrum, resulting in strong interaction and thus attenuation. In contrast, gold and lead attenuated the photons comparably weakly being in agreement with theory as the k-edges of these elements do not optimally match the effective energy of the spectrum at this voltage.

In relation, some elements could profit from higher voltages in terms of contrast generation. At a tube voltage of 90 kV, e.g., gadolinium, demonstrated the highest attenuation rate as it more favorably overlaps with the produced X-ray spectrum, followed by iodine and ytterbium as iodine and lanthanum decreased in attenuation efficiency. This can be attributed to the shift of the effective energy of the X-ray photon spectrum towards higher energies and a broadening of the overall spectrum at higher tube voltage. With increasing effective energy of the spectrum, ytterbium as a result showed a comparatively higher attenuation, whereas iodine and lanthanum decreased in attenuation efficiency. The heavy elements gold, lead, and bismuth continued to give the lowest attenuation rates.

At a tube voltage of 120 kV, gadolinium again exhibited the best contrasting properties whereas iodine, gold, bismuth, lanthanum, and lead displayed significantly lower attenuation rates. This is a result of the k-edge of gadolinium being close to the effective energy of the X-ray photon spectrum at 120 kV, resulting in considerable numbers of photons interacting with the contrast agent. This is also consistent with the results obtained for iodine and lanthanum, both displaying lower

attenuation rates in comparison as the effective energy of the X-rays moves away from their k-edges. Although the effective energy of the photons shifted to higher values, the heavy elements still could not profit in terms of contrast generation at 120 kV.

The relationship between the k-edge of the element and the energy of X-ray spectrum at a certain tube voltage is illustrated very well by the example of ytterbium. At tube voltages of 70 and 90 kV, ytterbium shows a considerably lower attenuation compared to gadolinium and iodine. At higher tube voltages, the effective energy of the spectrum increases, shifting towards the k-edge of ytterbium (61.3 keV), strongly increasing the contrasting properties of the element. The k-edges of the elements Pb and Bi, in comparison, lie at relatively higher energies of 88.0 keV and 90.5 keV, respectively), resulting in lower achievable contrasts. Another reason for the lower attenuation of the heavy elements is the k-edge absorption within the tungsten-based X-ray tube. In general, one would expect that the higher X-ray tube voltage would generate significantly more photons of higher energies, thus shifting the mean energy of the photons towards the k-edges of the heavy elements, resulting in strongly increasing attenuation rates of gold, lead and bismuth. Experimentally, it was found here that these elements indeed show increasing attenuation rates compared to iodine, gadolinium and ytterbium at 120 kV tube voltage but are still not able to compete with the latter in terms of achievable contrasts. These results are in agreement with studies performed on preclinical devices and early clinical PCCT prototypes [19,21]. Nevertheless, their use may still be indicated in cases when contrast agents with very different absorption behavior at different tube voltages are required for material decomposition imaging.

This study has certain limitations. In this study we carried out a systematic investigation on the comparative suitability of the individual elements for PCCT imaging – the application of these agents in humans and the associated quantities that are actually required go beyond the scope of our research question. However, the quantities we investigated for this purpose are unlikely to be necessary for in vivo imaging applications: A very recent experimental preclinical study using the approved iodine- and gadolinium-containing contrast agents iopamirone and magnescope in quantities of the same order of magnitude as in humans (based on body weight) demonstrated the differentiability of both agents within one PCCT scan [23]. Thus, multi-contrast PCCT imaging should be feasible within the range of the common clinical contrast agent quantities. This study aimed at the synthesis of new contrast agents and the determination of their contrasting properties in PCCT. Although all compounds were found to be highly stable and, due to their physical properties, are in principle suitable for in vivo PCCT imaging, the biological properties of the developed contrast agents have to be investigated as well prior to clinical application. This includes aspects such as biocompatibility including viscosity and osmolarity, but also, of course, detailed investigations of the acute and chronic toxicity of the compounds as well as the determination of the maximum tolerable substance amount. These issues are central for the safe clinical application of the substances and must be investigated in depth prior to human use.

Although the Naeotom Alpha PCCT system is approved for human application, the methodology and technology of the PCCT detectors are still under development and far from being fully developed. Thus, the quantitative results of the study may slightly differ using other scanners and with the introduction and continued development of new PCCT detectors. By now, this work represents the first study of multiple PCCT contrast agents based on stably encapsulated and thus in principle biocompatible form of lanthanum, ytterbium, lead, bismuth, and gold performed on a clinically approved device. It is possible that the scanner conditions may change slightly over the next few years and as a result, the here reported attenuation rates might show slight deviations. Another limitation are the energy thresholds of the PCCT detectors on the Naeotom Alpha scanner with currently two fixed thresholds and energy bins. With regard to k-edge imaging and material decomposition, energy bins adapted to the elements, with one energy bin with slightly lower energy and one energy bin with slightly higher energy than the k-edge of the respective element, are essential. At present, no clinical PCCT system with adjustable energy thresholds is available. All known studies with adjustable energy thresholds enabling binning and thus material decomposition enabling insights into biological processes have been performed on prototypes or preclinical scanners [34,35]. This is mainly due to the fact that there is currently no clinical need for manufacturers to offer corresponding energy binning for their systems, as no biocompatible and highly soluble contrast agents have been available to date that would have made material decomposition possible and thus required energy binning on the scanner side. This situation will change as a result of this work and future studies in this field, which is why the present work lays an important foundation for exploiting the full potential of PCCT in the future.

5. Conclusions

In summary, new and biocompatible contrast agents based on the elements lanthanum, gadolinium, ytterbium, gold, lead, and bismuth for use as contrast agents in PCCT were developed, synthesized and fully characterized with regard to chemical identity and stability. When examining the agents regarding their contrasting behavior in phantom studies on a clinical PCCT scanner, gadolinium and iodine demonstrated the highest attenuation of X-ray photons at 70 and 90 kV tube voltage whereas ytterbium and gadolinium showed the highest achievable contrasts at 120 and 140 kV. Accordingly, these elements are considered superior candidates for further contrast-enhanced studies and are also promising for further material decomposition and k-edge imaging studies. Nevertheless, as also gold and bismuth showed non-negligible contrasting properties at 140 kV, these elements would in principle be suitable for material decomposition studies in combination with the aforementioned iodine, gadolinium and ytterbium in cases where contrast agents with very different absorption behavior at different tube voltages are required.

The present study – together with other work to be expected in this field – will accelerate the further development of clinical PCCT systems toward energy binning, k-edge imaging and material decomposition and thus contribute to exploiting the full, extremely high potential of PCCT imaging clinically.

6. Human and animal rights

Not applicable.

7. Informed consent and patient details

Not applicable.

Authors contributions

All authors attest that they meet the current International Committee of Medical Journal Editors (ICMJE) criteria for authorship.

CRediT authorship contribution statement

Mika Donabauer: Writing – original draft, Formal analysis, Data curation, Conceptualization. **Stefan Sawall:** Writing – original draft, Formal analysis, Data curation, Conceptualization. **Isabelle Ayx:** Writing – review & editing, Formal analysis, Data curation, Conceptualization. **Carmen Wängler:** Writing – original draft, Project administration, Conceptualization. **Stefan O. Schoenberg:** Writing – review & editing, Conceptualization. **Björn Wängler:** Writing – review & editing, Project administration.

Funding

This work is part of the Research Campus M^2OLIE and was supported

by the German Federal Ministry of Education and Research (BMBF) within the framework "Research Campus – public–private partnership for Innovation" under the funding codes 13GW0389B and 13GW0388A. Further, this work was supported by the Deutsche Forschungsgemeinschaft (DFG) under project number 394,046,768 – SFB 1366 Z02.

Declaration of competing interest

The authors have no conflicts of interest to declare.

Appendix A. Supplementary data

Supplementary data to this article can be found online at https://doi.org/10.1016/j.ejrad.2025.112643.

References

[1] L. Schöckel, G. Jost, P. Seidensticker, P. Lengsfeld, P. Palkowitsch, H. Pietsch, Developments in X-Ray contrast media and the potential impact on computed tomography, Invest. Radiol. 55 (9) (2020) 592–597.
[2] H. Lusic, M.W. Grinstaff, X-ray-computed tomography contrast agents, Chem. Rev. 113 (3) (2013) 1641–1666.
[3] J.A. Seibert, X-ray imaging physics for nuclear medicine technologists. Part 1: basic principles of x-ray production, J. Nucl. Med. Technol. 32 (3) (2004) 139–147.
[4] J.A. Seibert, J.M. Boone, X-ray imaging physics for nuclear medicine technologists. Part 2: X-ray interactions and image formation, J. Nucl. Med. Technol. 33 (1) (2005) 3–18.
[5] B.M. Yeh, P.F. FitzGerald, P.M. Edic, J.W. Lambert, R.E. Colborn, M.E. Marino, et al., Opportunities for new CT contrast agents to maximize the diagnostic potential of emerging spectral CT technologies, Adv. Drug Deliv. Rev. 113 (2017) 201–222.
[6] M.J. Willemink, M. Persson, A. Pourmorteza, N. Pelc, D. Fleischmann, Photon-counting CT: technical principles and clinical prospects, Radiology 289 (2) (2018) 293–312.
[7] H. Gomes, M.M. Jaseemudheen, Photon-counting detectors in computed tomography: a review, JHASNU 13 (2) (2023) 147–152.
[8] Y. Nakamura, T. Higaki, S. Kondo, I. Kawashita, I. Takahashi, K. Awai, An introduction to photon-counting detector CT (PCD CT) for radiologists, Jpn. J. Radiol. 41 (3) (2023) 266–282.
[9] M. Danielsson, M. Persson, M. Sjölin, Photon-counting x-ray detectors for CT, Phys. Med. Biol. 66 (3) (2021).
[10] D. Richtsmeier, C.A.S. Dunning, K. Iniewski, M. Bazalova-Carter, Multi-contrast K-edge imaging on a bench-top photon-counting CT system: acquisition parameter study, J. Instrum. 15 (10) (2020) P10029.
[11] T. Flohr, M. Petersilka, A. Henning, S. Ulzheimer, J. Ferda, B. Schmidt, Photon-counting CT review, Phys. Med. 79 (2020) 126–136.
[12] R. Solem, T. Dreier, I. Goncalves, M. Bech, Material decomposition in low-energy micro-CT using a dual-threshold photon counting X-Ray detector, Front. Phys. 9 (2021) 673843.
[13] K. Treb, R. Zhang, G.-H. Chen, K. Li, K-edge photon counting CT imaging using a dual-bin photon counting detector an kV switching, Proc. SPIE 12463 (2023) 1246331.
[14] S. Si-Mohamed, S. Boccalini, P.A. Rodesch, R. Dessouky, E. Lahoud, T. Broussaud, et al., Feasibility of lung imaging with a large field-of-view spectral photon-counting CT system, Diagn. Interv. Imaging 102 (5) (2021) 305–312.
[15] S.A. Si-Mohamed, J. Miailhes, P.A. Rodesch, S. Boccalini, H. Lacombe, V. Leitman, et al., Spectral photon-counting CT technology in chest imaging, J. Clin. Med. 10 (24) (2021) 5757.
[16] P.C. Douek, S. Boccalini, E.H.G. Oei, D.P. Cormode, A. Pourmorteza, L. Boussel, et al., Clinical applications of photon-counting CT: a review of pioneer studies and a glimpse into the future, Radiology 309 (1) (2023) e222432.
[17] S. Si-Mohamed, V. Tatard-Leitman, A. Laugerette, M. Sigovan, D. Pfeiffer, E. J. Rummeny, et al., Spectral Photon-counting Computed Tomography (SPCCT): in-vivo single-acquisition multi-phase liver imaging with a dual contrast agent protocol, Sci. Rep. 9 (1) (2019) 8458.
[18] Hubbell J, Seltzer S. Tables of X-ray mass attenuation coefficients and mass engery-absorption coefficients 1 keV to 20 MeV for elements Z = 1 to 92 and 48 additional substances of dosimetric interest. 1995. DOI: 10.18434/T4D01F.
[19] Y.C. Dong, A. Kumar, D.N. Rosario-Berríos, S. Si-Mohamed, J.C. Hsu, L.M. Nieves, et al., Ytterbium nanoparticle contrast agents for conventional and spectral photon-counting CT and their applications for hydrogel imaging, ACS Appl. Mater. Interfaces 14 (34) (2022) 39274–39284.
[20] M. Moghiseh, C. Lowe, J.G. Lewis, D. Kumar, A. Butler, N. Anderson, et al., Spectral photon-counting molecular imaging for quantification of monoclonal antibody-conjugated gold nanoparticles targeted to lymphoma and breast cancer: an in vitro study, Contrast Media Mol. Imaging (2018).
[21] J. Kim, D. Bar-Ness, S. Si-Mohamed, P. Coulon, I. Blevis, P. Douek, et al., Assessment of candidate elements for development of spectral photon-counting CT specific contrast agents, Sci. Rep. 8 (2018) 12119.
[22] C. Amato, L. Klein, E. Wehrse, L.T. Rotkopf, S. Sawall, J. Maier, et al., Potential of contrast agents based on high-Z elements for contrast-enhanced photon-counting computed tomography, Med. Phys. 47 (12) (2020) 6179–6190.
[23] D. Sato, M. Arimoto, A. Ishiguro, F. Lucyana, T. Tomoda, K. Okumura, et al., Multi-energy in-vivo imaging of multiple contrast agents in a mouse using MPPC-based photon-counting CT, Nucl Instrum Meth A 1064 (2024) 169337.
[24] C. Amato, M. Susenburger, S. Lehr, J. Kuntz, N. Gehrke, D. Franke, et al., Dual-contrast photon-counting micro-CT using iodine and a novel bismuth-based contrast agent, Phys. Med. Biol. 68 (13) (2023) 135001.
[25] W.P. Cacheris, S.C. Quay, S.M. Rocklage, The relationship between thermodynamics and the toxicity of gadolinium complexes, Magn. Reson. Imaging 8 (4) (1990) 467–481.
[26] M.S. Collin, S.K. Venkatraman, N. Vijayakumar, V. Kanimozhi, S.M. Arbaaz, R.G. S. Stacey, et al., Bioaccumulation of lead (Pb) and its effects on human: a review, J Hazard Mater Adv 7 (2022) 100094.
[27] J. Wahsner, E.M. Gale, A. Rodríguez-Rodríguez, P. Caravan, Chemistry of MRI contrast agents: current challenges and new frontiers, Chem. Rev. 119 (2) (2019) 957–1057.
[28] C. Zhou, M. Long, Y.P. Qin, X.K. Sun, J. Zheng, Luminescent gold nanoparticles with efficient renal clearance, Angew. Chem. Int. Ed. 50 (14) (2011) 3168–3172.
[29] M.F. Ferreira, J. Gonçalves, B. Mousavi, M.I.M. Prata, S.P.J. Rodrigues, D. Calle, et al., Gold nanoparticles functionalised with fast water exchanging Gd3+ chelates: linker effects on the relaxivity, Dalton Trans. 44 (9) (2015) 4016–4031.
[30] N.R. Jana, C. Earhart, J.Y. Ying, Synthesis of water-soluble and functionalized nanoparticles by silica coating, Chem. Mater. 19 (21) (2007) 5074–5082.
[31] M.Z. Xu, Y.M. Qi, G.S. Liu, Y.Q. Song, X.Y. Jiang, B.J. Du, Size-dependent in vivo transport of nanoparticles: implications for delivery, targeting, and clearance, ACS Nano 17 (21) (2023) 20825–20849.
[32] M. Magerstadt, O.A. Gansow, M.W. Brechbiel, D. Colcher, L. Baltzer, R.H. Knop, et al., Gd(Dota) - an Alternative to Gd(Dtpa) as a T1,2 relaxation agent for nmr imaging or spectroscopy, Magn Res Med 3 (5) (1986) 808–812.
[33] M. Allard, D. Doucet, P. Kien, B. Bonnemain, J.M. Caille, Experimental-study of dota-gadolinium pharmacokinetics and pharmacologic properties, Invest. Radiol. 23 (1988) S271–S274.
[34] R. Symons, B. Krauss, P. Sahbaee, T.E. Cork, M.N. Lakshmanan, D.A. Bluemke, et al., Photon-counting CT for simultaneous imaging of multiple contrast agents in the abdomen: an in vivo study, Med. Phys. 44 (10) (2017) 5120–5127.
[35] C.T. Badea, D.P. Clark, M. Holbrook, M. Srivastava, Y. Mowery, K.B. Ghaghada, Functional imaging of tumor vasculature using iodine and gadolinium-based nanoparticle contrast agents: a comparison of spectral micro-CT using energy integrating and photon counting detectors, Phys. Med. Biol. 64 (6) (2019) 065007.